International Immunopharmacology 81 (2020) 106270

Contents lists available at ScienceDirect

International Immunopharmacology

journal homepage: www.elsevier.com/locate/intimp

Effect of berberine on spleen transcriptome and gut microbiota composition in experimental autoimmune uveitis

Ziyu Du[a], Qingfeng Wang[a], Xinyue Huang[a], Shenglan Yi[a], Suyin Mei[a], Gangxiang Yuan[a], Guannan Su[a], Qingfeng Cao[a], Chunjiang Zhou[a], Yao Wang[a], Aize Kijlstra[b], Peizeng Yang[a,*]

[a] The First Affiliated Hospital of Chongqing Medical University, Chongqing Key Laboratory of Ophthalmology and Chongqing Eye Institute, Chongqing, PR China
[b] University Eye Clinic Maastricht, Maastricht, Limburg, the Netherlands

ARTICLE INFO

Keywords:
Berberine
Experimental autoimmune uveitis
Transcriptome
Gut microbiota

ABSTRACT

Background: Berberine (BBR) was reported to have immunoregulatory and anti-inflammatory properties. In this study, we investigated whether BBR could exert its effects on the development of experimental autoimmune uveitis (EAU), and if so, what was the underlying mechanism?

Methods: EAU was induced in B10R.III mice by immunization with IRBP 161–180, followed by 100 mg/kg/d BBR intragastric administration. Disease severity was assessed by evaluation of clinical and histopathological scores. Blood-retinal barrier (BRB) breakdown was tested by Evans blue. Effector and regulatory T (Treg) cell balance was evaluated by quantitative real-time PCR and flow cytometry. Spleen transcriptome was characterized by RNA sequencing (RNA-seq). Gut microbiota composition was investigated by 16S rRNA analysis.

Results: BBR treatment significantly blocked EAU as shown by the decrease of the clinical and histological scores, as well as the inhibition of BRB breakdown. The frequency of splenic Th1 and Th17 cells was decreased, whereas Treg cells were increased in the BBR-treated group. RNA-seq of the spleen revealed 476 differentially expressed genes (DEGs) between the EAU and EAU-BBR group. GO functional classification, as well as KEGG analysis demonstrated that BBR treatment markedly influences genes belonging to chromatin remodeling and immune-related pathways. Intervention with BBR modified the gut microbiome in EAU mice, increasing the number of bacteria with immunomodulatory capacity. Depletion of gut microbiota affected the efficacy of BBR on EAU. Moreover, the altered bacterial strains showed a significant correlation with the expression of histones.

Conclusions: BBR inhibited IRBP induced EAU, which was associated with a significant change in the spleen transcriptome and intestinal microbial composition.

1. Introduction

Uveitis is a blinding intraocular inflammatory disease occurring in the uveal layers, although other intraocular tissues such as the retina and vitreous may also be involved. It is often caused by an autoimmune response and clinical uveitis is often associated with a systemic immune dysregulation leading to intraocular inflammatory disease as seen in patients with Behcet's disease (BD) or Vogt-Koyanagi-Harada (VKH) disease [1]. The current treatment for autoimmune uveitis is primarily dependent on the systemic use of steroids and immunosuppressive drugs [2]. Nevertheless, the use of these medications is often limited due to their serious side effects [3]. Therefore, there is an urgent need to develop novel drugs with a lower toxicity.

Experimental autoimmune uveitis (EAU) has been developed as a widely used model of clinical uveitis in humans, and can be induced by immunization with retinal-specific antigens in the presence of strong adjuvants [4]. IRBP 161–180 peptide-induced EAU in B10R.III mice shows an acute and severe inflammation involving both the anterior and posterior segments of the eye and is a good model for human panuveitis [5]. Autoreactive retina-specific T cells which secrete IFN-γ or IL-17A are generated in lymph nodes and spleen and cross the blood-retinal barrier (BRB), whereafter inflammatory cells are recruited into the retina that eventually leads to full blown uveoretinal inflammation [6,7].

BBR is an isoquinoline alkaloid extracted from many medicinal Chinese herbs, such as Cortex phellodendri, Hydrastis canadensis and Rhizoma coptidis, It has been used widely as an antibacterial and anti-inflammatory therapy with a good safety profile, although its precise mechanisms of action remain to be elucidated [8]. Interestingly, BBR was also found to have immunomodulatory effects in several

* Corresponding author at: The First Affiliated Hospital of Chongqing Medical University, Youyi Road 1, Chongqing 400016, PR China.
E-mail address: peizengycmu@126.com (P. Yang).

https://doi.org/10.1016/j.intimp.2020.106270
Received 1 November 2019; Received in revised form 18 January 2020; Accepted 29 January 2020

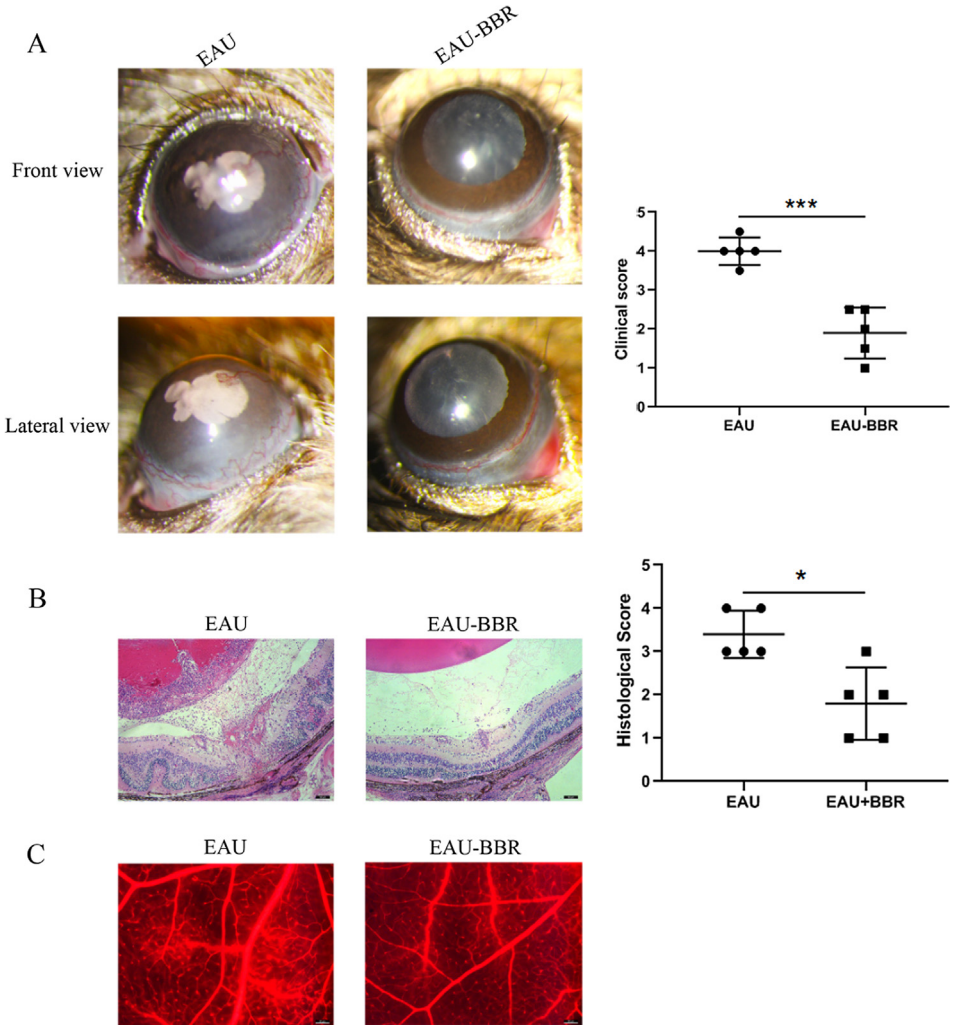

Fig. 1. Ocular evaluation of EAU mice: BBR intragastric administration reduced the clinical scores, histological scores and inhibited BRB breakdown in EAU mice. (A) Left, representative slit-lamp images of eye sections in EAU and BBR treated EAU mice. Right, quantification of clinical scores (n = 5/group; mean ± SD; ***p < 0.001; Unpaired *t*-test). (B) Left, representative hematoxylin and eosin images of eye sections from EAU and BBR treated EAU mice. Right, quantification of histopathological score s(n = 5/group; mean ± SD; *p < 0.05; Mann-Whitney *U* test). (C) Representative Evans blue images of retinas from EAU or BBR treated EAU mice. Scale bar, 80 μm (n = 5/group). Representative data from 3 to 4 independent experiments. (For interpretation of the references to colour in this figure legend, the reader is referred to the web version of this article.)

autoimmune diseases [9]. In a model of ulcerative colitis, BBR treatment decreased inflammatory cells and increased Tregs which was associated with a change in the composition of the intestinal microbiota [10]. In an experimental model of multiple sclerosis, treatment with BBR ameliorated disease by decreasing nervous system (CNS) and spleen infiltrating effector T cells [11]. An earlier study demonstrated that BBR suppresses Th17 responses in ocular Behcet's disease and Vogt-Koyanagi-Harada disease patients in vitro [12,13]. The exact role of BBR in uveitis is however not yet clear and was therefore the purpose of our study whereby we studied the effect of BBR on uveitis in an animal model (EAU) and investigated the possible underlying mechanisms. BBR had an inhibitory effect on EAU, which was associated with marked changes in the splenic transcriptome and gut microbiota composition.

2. Methods

2.1. BBR and animals

BBR hydrochloride (C20H18NO4 + Cl-) (purity > 95%) was obtained from Sigma-Aldrich (CAS NO: 633-65-8, St. Louis, MO, USA), and it is endotoxin-free. B10RIII mice were obtained from Jackson Laboratory (Bar Harbor, ME) and kept under specific pathogen free conditions at the Animal Care Service of Chongqing Medical University. Animal experiments were performed according to the Association for Research in Vision and Ophthalmology (ARVO) statement for the use of Animals in Ophthalmic and Vision Research. The Ethics Committee of the First Affiliated Hospital of Chongqing Medical University approved all the protocols of this study.

2.2. Induction of EAU

Interphotoreceptor retinoid binding protein (IRBP) peptide 161–180 (IRBP161–180, SGIPYIISYLHPGNTILHVD) was synthesized by Shanghai Sangon (Shanghai, China). EAU was induced in B10RIII mice with an emulsion including 50 μg IRBP161-180 in complete Freund's adjuvant (CFA, Sigma-Aldrich, St. Louis, MO, USA). For treatment, BBR or double distilled H2O (ddH2O) was administered intragastrically at 100 mg/kg daily, starting from the day of immunization and continuing thereafter for 14 days.

2.3. Depletion of the gut microbiota

Mice were were treated with an antibiotic cocktail containing ampicillin (1 mg/ml), neomycin (1 mg/ml), metronidazole (1 mg/ml), and vancomycin (0.5 mg/ml) (all purchased from Sigma-Aldrich, St. Louis, MO, USA) in their drinking water for 3 weeks and continued for the duration of the experimentas.

2.4. Clinical and histological scores

Clinical signs of EAU were assessed by slit-lamp microscopy and the severity was scored on a scale of 0–5. Eyes were enucleated at day 14 post-immunization [14]. They were fixed in 4% glutaraldehyde, and

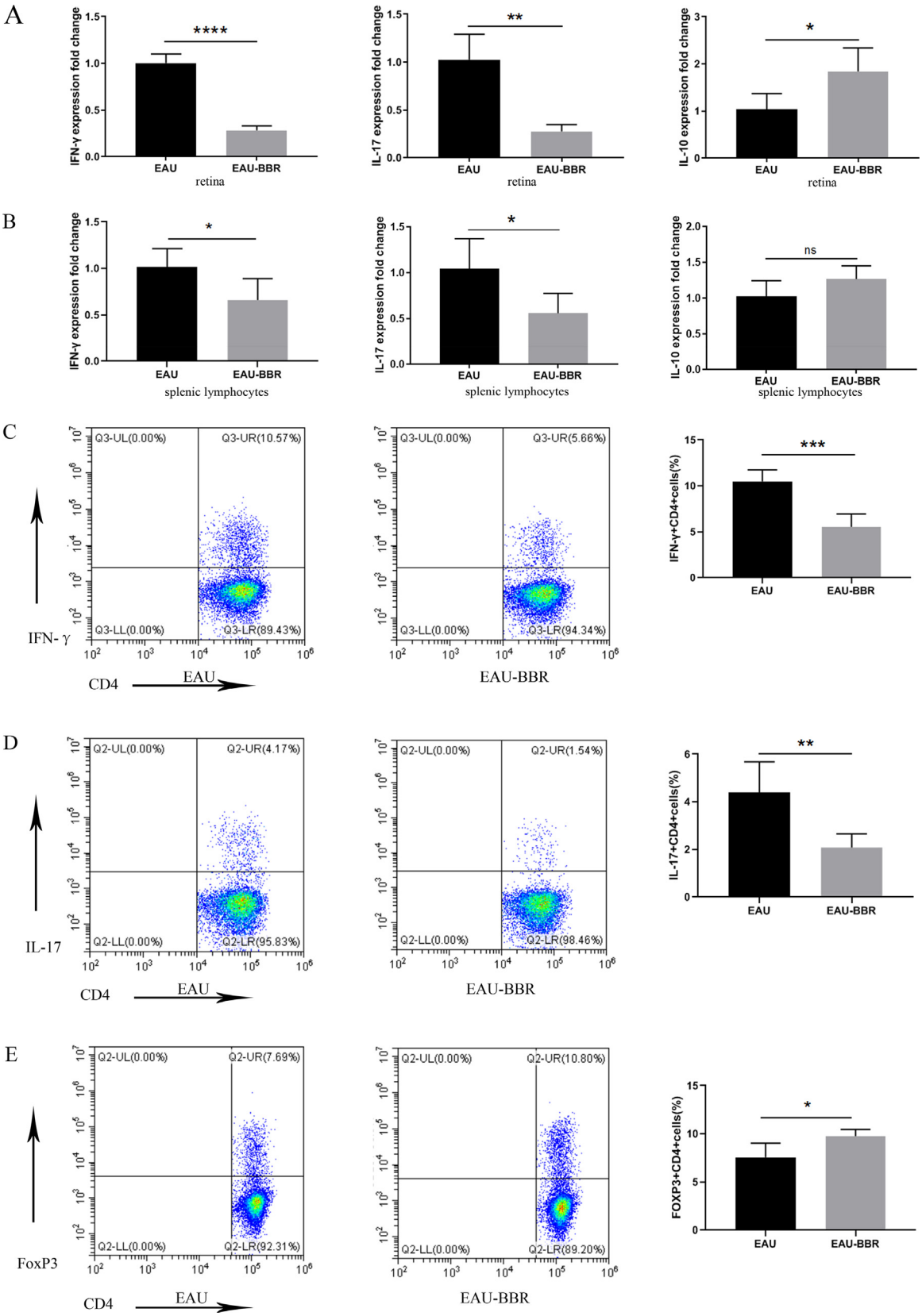

Fig. 2. BBR treatment alters effector and regulatory T cell balance in EAU mice. (A) The mRNA expression of IFN-γ, IL-17, IL-10 were detected by real-time PCR in retina from EAU and EAU-BBR mice. (n = 5/group; mean ± SD; **** $p < 0.0001$, ** $p < 0.01$, *$p < 0.05$; Unpaired *t*-test or Mann-Whitney *U* test). (B) The mRNA expression of IFN-γ, IL-17, IL-10 were detected by real-time PCR in splenic lymphocytes from EAU and EAU-BBR mice. (n = 5/group; mean ± SD; *$p < 0.05$; Unpaired *t*-test). (C–E) Representative and quantification of IFN-γ + CD4 + T cells, IL-17A + CD4 + T cells and CD4 + Foxp3 + cells in the splenic lymphocytes of EAU mice. (n = 5/group; mean ± SD; ***$p < 0.001$; **$p < 0.01$; *$p < 0.05$; Unpaired *t*-test). Representative data from 3 to 4 independent experiments.

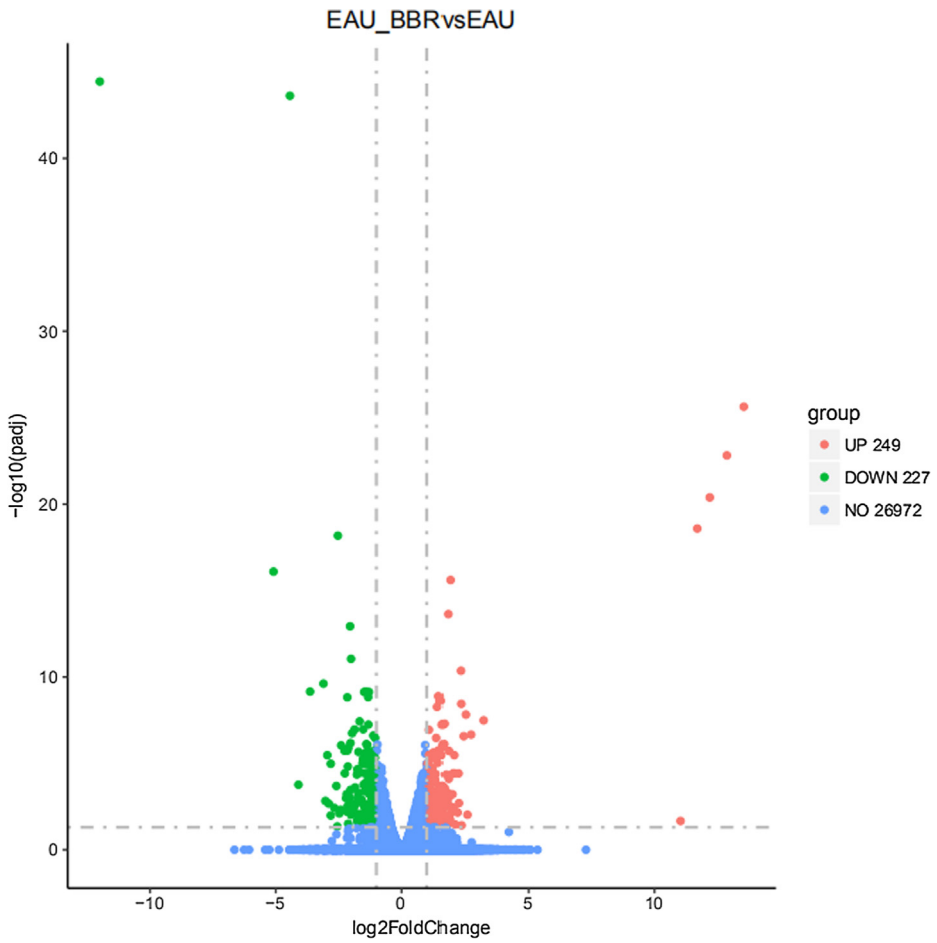

Fig. 3. Transcriptomic analyses of EAU and EAU-BBR group mice spleens. (A). Volcano plot of the up and downregulated DEGs. The number of the differential genes between the EAU and EAU-BBR group are shown in the volcano plots. The horizontal axis is log2-fold change, and the vertical lines indicate the statistical significance of the different gene expression levels. The red dots indicate the upregulated genes, whereas the green dots represent the downregulated genes. The corrected P < 0.05, |log2foldchange| > 1 was an absolute threshold used to select DEGs. DEGs, differentially expressed genes. (B) GO analysis of the DEGs identified in the spleens between the EAU group and the EAU-BBR group. DEGs were classified into the three categories of the GO classification (biological processes, molecular functions and cellular components), and the numbers of DEGs and their percentages are presented on the left and right axes, respectively. (C) The top 20 downregulated KEGG pathways associated with the identified DEGs between the EAU group and the EAU-BBR group. The horizontal axis and the vertical axis indicate the log (corrected P value) and the function descriptions of the enriched pathways, respectively. The corrected P < 0.05 was an absolute threshold used to select significantly enriched pathways (*adjusted P value < 0.05). KEGG, Kyoto Encyclopedia of Genes and Genomes. (For interpretation of the references to colour in this figure legend, the reader is referred to the web version of this article.)

embedded in paraffin. Tissue sections were stained with hematoxylin and eosin. Histological inflammation was graded on a scale from 0 to 4, as described earlier [15].

2.5. Evans blue

Evans blue (EB) was used to evaluate the microvascular permeability of the BRB [16]. Briefly, 100 μl of 2% EB (Sigma-Aldrich, St. Louis, MO, USA) was injected into mice via the tail veins. After 2 h, the mice were sacrificed, their eyes were enucleated and fixed in 4% glutaraldehyde for 2 h. Retinal whole mounts were prepared and an immunofluorescent microscope (Leica, Germany) was used to examine EB leakage.

2.6. Real time PCR analysis

EAU mice were sacrificed and spleens and retina were harvested 14 days post primary immunization. Splenic cell suspensions were obtained by processing through a cell mesh. Cells were suspended in a lymphocyte separating medium and washed twice with PBS. Total RNA was isolated from the splenic lymphocytes or retina tissue using Trizol Reagent (Invitrogen, Carlsbad, USA). cDNA was synthesized using Prime Script RT reagent Kit (Takara Biotechnology, Dalian, China). The expression of IL-17, IFN-γand IL-10 was detected by real-time PCR using SYBR Green Master Mix (Takara Biotechnology, Dalian, China). The primers are listed in Table S1.

2.7. Flow cytometry

The frequency of regulatory T cells (Treg) in the splenic cell suspensions was determined after staining with a specific anti-mouse T helper cell antibody: CD4-APC, (BioLegend, San Diego, CA). Foxp3/Transcription Factor Staining Buffer Set (eBioScience, San Diego, CA) was then used to fix the cells, followed by staining with anti-mouse FoxP3-PE (BioLegend, San Diego, CA). For Th1 and Th17 cell assessment, suspensions of splenic cells were stimulated for 5 h with the cell activation cocktail (BioLegend, San Diego, CA), which includes an optimized concentration of PMA (phorbol 12-myristate-13-acetate), ionomycin, and protein transport inhibitor (Brefeldin A). The stimulated cells were stained with an anti-mouse CD4-APC (BioLegend, San Diego, CA) antibody and then fixed with Fix/Perm buffer (BioLegend, San Diego, CA) prior to staining with the anti-mouse antibodies: IFNγ-PE/

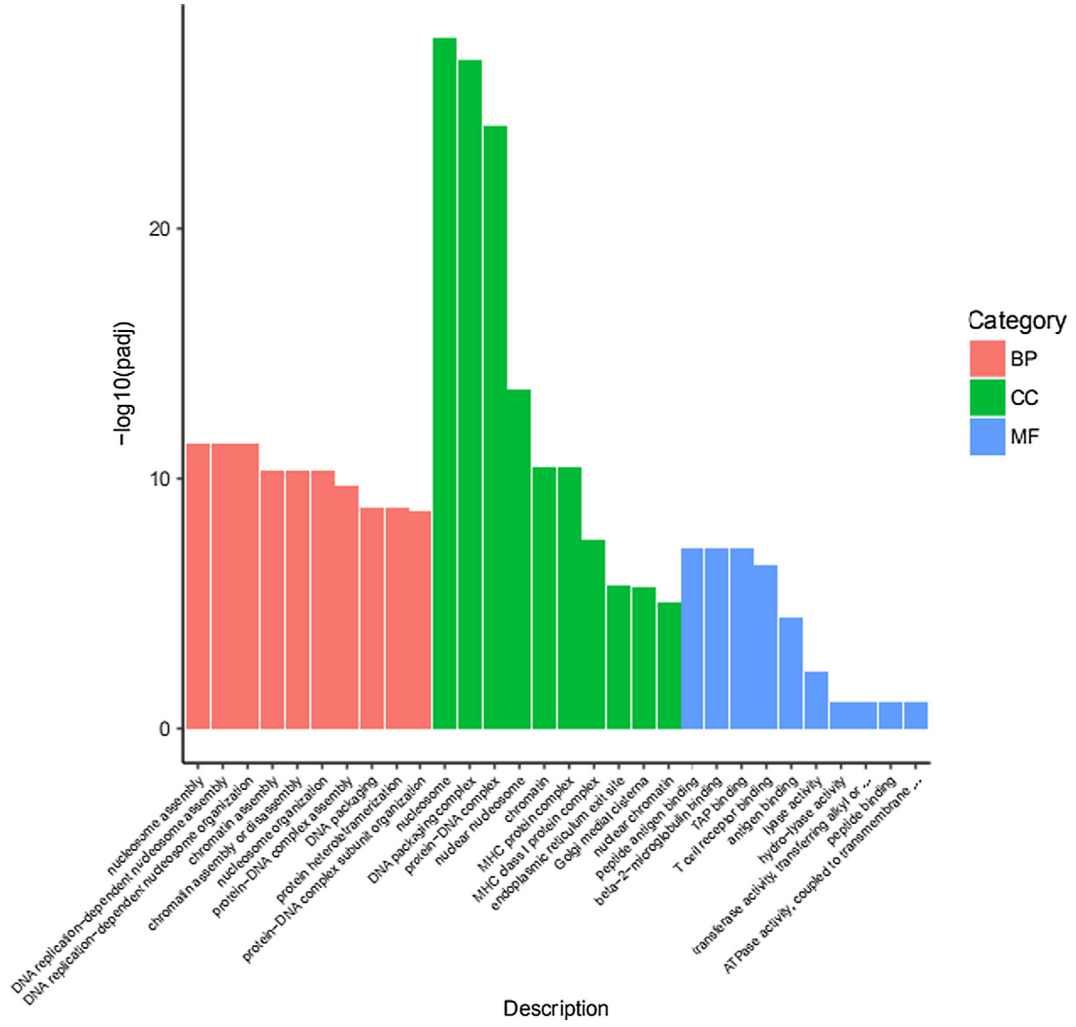

Fig. 3. (*continued*)

Cy7 (BioLegend, San Diego, CA), or IL-17A-PE (BioLegend, San Diego, CA). Flow cytometric data after dual staining were obtained with a CytoFLEX flow cytometer (Beckman Coulter, California, USA). Data were analyzed usingCytExpert software (Beckman Coulter, California, USA) with a total of 10,000 events being recorded for each sample through a live, single-cell CD4+ gate [17].

2.8. RNA-seq

Spleens from three randomly selected EAU mice from the ddH2O-treated control group and the 100 mg/kg/d BBR-treated group were subjected to RNA-Seq. Total RNA was isolated from the spleen using Trizol Reagent. RNA contamination and degradation were checked on agarose gels. A NanoDrop2000 spectrophotometer (IMPLEN, CA, USA) was used to monitor the RNA purity. The Qubit® RNA Assay Kit and Qubit®2.0 Fluorimeter (Life Technologies, CA, USA) was used to assess the RNA concentration. The RNA Nano 6000 Assay Kit of the Bioanalyzer 2100 system (Agilent Technologies, CA, USA) was used to measure RNA integrity. cDNA was synthesized using the NEBNext® UltraTM RNA Library Prep Kit for Illumina® (NEB, USA). The Illumina Novaseq 6000 platform (Shanghai Bio-tree Technology Co. Ltd, Shanghai, China) was used to perform RNA sequencing. Quality control of raw reads enabled the downstream analysis to be based on clean reads with high quality. Hisat2 v2.0.5 (http://www.ccb.jhu.edu/software/hisat/) was used to build an index of the reference genome and to compare paired-end clean reads of the reference genome. FPKM (Fragments Per Kilobase per Million) were calculated to measure gene expression level by feature Counts v1.5.0-p3 (http://subread.sourceforge.net).

DEGs were analyzed with the DESeq2 R package (1.16.1) (http://www.bioconductor.org/packages/release/bioc/html/DESeq2.html).

The Benjamini-Hochberg false discovery rate (FDR) was used to adjust P-values. Genes with FDR $<$ 0.05 and $|\log2foldchange| > 1$ were seen as significantly differentially expressed. ClusterProfiler R package (http://bioconductor.org/packages/release/bioc/html/clusterProfiler.html) was used to perform Gene Ontology (GO) enrichment analysis of DEGs. Kyoto Encyclopedia of Genes and Genomes (KEGG) pathway analysis and functional annotation for differential genes were also implemented by the clusterProfiler R package. An absolute threshold corrected P $<$ 0.05 was taken for significantly enriched GO terms and pathways.

Experimental validation of specific genes was performed by qRT-PCR using total RNA isolated from mouse spleen, with methods of RNA extraction, DNA synthesis and RT-PCR as described above. The primers used are shown in Table S1.

2.9. Feces DNA extraction and 16S rRNA sequencing

Feces was collected from mice after 14 days of treatment. The CTAB (cetyltrimethyl ammonium bromide)/SDS (sodium dodecyl sulfate) method was used to extract bacterial DNA from the feces [18]. The V4 16S rRNA region was amplified, using universal primers 341F/806R. Phusion® High-Fidelity PCR Master Mix (New England Biolabs) was used to perform PCR reactions. TruSeq® DNA PCR-Free Sample

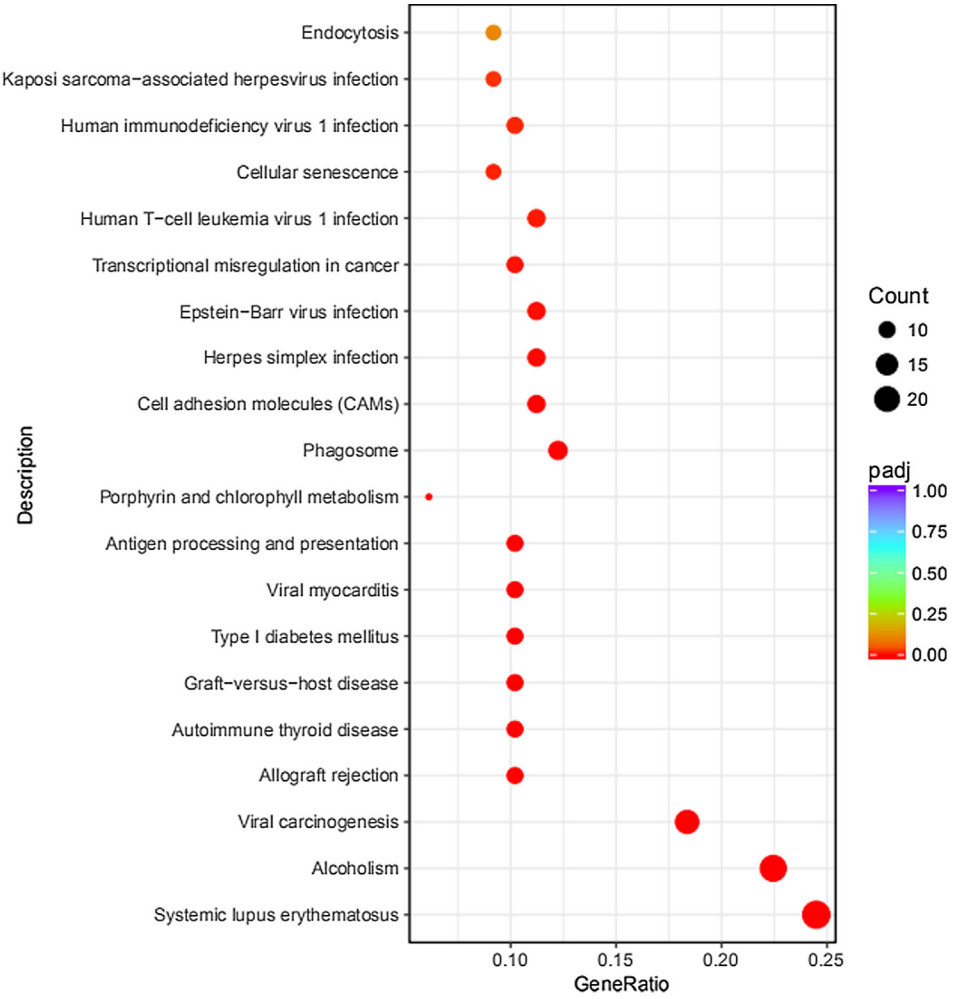

Fig. 3. (*continued*)

Table 1
The selected gene ontology terms from significantly downregulated GO terms and KEGG pathways.

Ensgene	Gene symbol	log2-fold change	padj	Description
ENSMUSG00000073411	H2-D1	−2.0450	1.14E-13	histocompatibility 2, D region locus 1
ENSMUSG00000069273	Hist1h3e	−1.6988	8.74E-03	histone cluster 1, H3e
ENSMUSG00000022797	Tfrc	−1.5548	9.98E-06	transferrin receptor
ENSMUSG00000066687	Zbtb16	−1.1076	4.77E-03	zinc finger and BTB domain containing 16
ENSMUSG00000025408	Ddit3	−1.005	6.65E-05	DNA-damage inducible transcript 3

Preparation Kit (Illumina, USA) was used to generate sequencing libraries. Illumina HiSeq 2500 platform was used to perform 16S rRNA sequencing. QIIME was used to obtain the high-quality clean reads from raw reads [19]. UCHIME was used to filter chimeric sequences [20]. Operational taxonomic units (OTU) data were summarized by using Uparse software [21]. Species annotation was performed by Silva Database [22]. Alpha and beta diversity were calculated by QIIME. Analysis of similarity (ANOSIM) was performed to determine the differences among groups. Linear discriminant analysis (LDA) of effect size (LEfSe) was assessed with the LEfSe tool [23]. Flora relative abundance between samples were compared by metastat analysis [24].

2.10. Statistical analysis

Statistical calculations were performed using SPSS software 19.0 (IBM, USA). Student's *t*-test or the Mann-Whitney *U* test was used for two-group comparisons. Two-way ANOVA with Tukey multiple comparisons test was used for four-group comparisons. A $P < 0.05$ was considered as significantly different. Prism version 8.0 software (GraphPad, San Diego, CA, USA) was used to make the statistical figures.

3. Results

3.1. BBR attenuates ocular manifestations of EAU

To determine whether BBR has an effect on the development of EAU, we induced EAU and treated the mice with BBR or the ddH2O vehicle control. Anterior chamber inflammation was examined by slit lamp. The ddH2O-treated EAU mice developed significant inflammation with clinical scores between 3.5 and 4.5, characterized by corneal edema, ciliary injection of the cornea, and cells in the aqueous humor as well as posterior synechiae. The clinical scores of the BBR-treated group ranged between 1 and 2.5, as manifested by conjunctival and/or ciliary injection, and slight corneal edema. The BBR-treated group showed a significantly lower clinical manifestation than the ddH2O-treated group

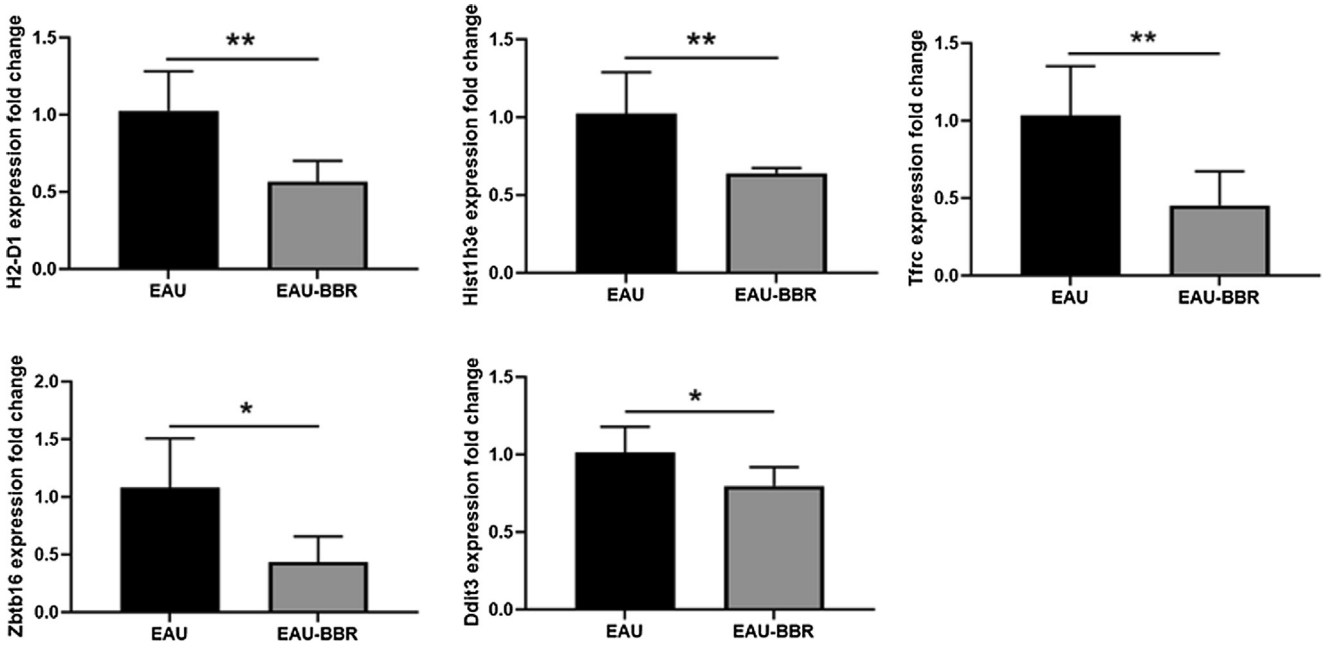

Fig. 4. Validation of DEGs with real-time quantitative PCR. These five genes were selected from the downregulated DEGs, and they were not only enriched in the significantly down-regulated GO terms, but also in the significantly down-regulated KEGG pathways. Compared with the EAU group, the mRNA expressions of H2-D1, Hist1h3e, Tfrc, Zbtb16, Ddit3 were remarkably decreased in the EAU-BBR group. The endogenous reference gene β-Actin was applied to normalize the relative expression of mRNA (n = 5/group; mean ± SD; *P < 0.05, **P < 0.01; Unpaired *t*-test or Mann Whitney text, representative data from 3 independent experiments).

(Fig. 1A).

Treatment with BBR also significantly attenuated the histological scores (Fig. 1B). EAU group mice showed obvious histological characteristics of uveitis, including massive inflammatory cells in the choroid and retina, retinal folds, and damage of photoreceptor cells. The BBR group of mice only showed slight retinal folding and the sporadic presence of inflammatory cells. Statistical analysis showed that the histological scores were significantly decreased in the EAU-BBR group mice as compared to the vehicle control group of EAU mice.

As shown in Fig. 1C. retinal Evans blue (EB) staining to evaluate BRB breakdown revealed a diffuse and widespread EB leakage from retinal vessels in EAU mice, whereas BBR inhibit the EB leakage, showing that BBR treatment also attenuated BRB breakdown in EAU.

3.2. BBR treatment alters effector and regulatory T cell balance

The effector and regulatory T cell balance in the retina was measured by PCR. The results showed that the mRNA expression of IFN-γ and IL-17 was significantly decreased in the EAU-BBR group, and the expression of IL-10 was markedly increased (Fig. 2A). To investigated whether BBR can regulate the systemic autoimmune response during EAU development, we measured Th1, Th17 and Treg activities in the spleen by PCR and flow cytometry assays. PCR results showed that the mRNA expression of IL-17 and IFN-γ was significantly decreased in the EAU-BBR group, while the expression of IL-10 only showed a slight increase, which was not statistically significant (Fig. 2B). We also measured the frequency of Th1 (IFN-γ + CD4 +), Th17 (IL-17 + CD4 +) and Treg cells (Foxp3 + CD4 +) in the two groups by flow cytometry. The frequency of Th1 and Th17 cells was significantly reduced in the EAU-BBR group compared to the untreated EAU group (Fig. 2C and 2D). On the other hand, the BBR-treated group showed a markedly increased frequency of Treg cells (Fig. 2E).

Fig. 2

3.3. Transcriptomic analysis of the spleen

To investigate the changes of spleen gene expression between the untreated EAU and BBR-treated EAU mice, RNA-seq was performed. Genes with an FDR < 0.05 and a log2 fold change > 1 were considered DEGs. The results showed that 476 genes were differentially expressed in the EAU group compared to the BBR-EAU group, whereby 249 DEGs were upregulated and 227 DEGs were downregulated (Fig. 3A). The results showed that treatment with BBR induced marked changes in the global gene transcription profiles.

The GO annotations of the DEGs involved three major categories: biological processes, cellular components, and molecular function. An absolute threshold of the corrected P < 0.05 was applied to select 3 significantly upregulated and 72 downregulated GO terms. The 3 upregulated GO term all belong to cellular component categories including basement membrane, extracellular matrix and collagen-containing extracellular matrix. The downregulated categories of the biological processes mainly including nucleosome assembly, chromatin assembly, myeloid cell differentiation and antigen processing and presentation. The downregulated cellular component categories mainly including nucleosome, DNA packaging complex, protein-DNA complex, nuclear nucleosome, chromatin and MHC protein complex. The downregulated categories of molecular function mainly included peptide antigen binding, beta-2-microglobulin binding and TAP binding, followed by T cell receptor binding, antigen binding and lyase activity. The top 30 GO terms are shown in Fig. 3B. It shows that BBR may play an anti-inflammatory role by downregulating splenic gene expression in EAU mice which include chromatin remodeling and immune response related GO terms.

Using KEGG pathway analysis we identified pathways that may be involved in the therapeutic mechanisms of BBR on EAU. The results showed that 20 significantly downregulated enriched pathways in the aggregate were found in the EAU group compared to the BBR-EAU group (Fig. 3C). The only upregulated pathway was the ECM-receptor interaction.

To confirm the differential gene expression results from RNA seq,

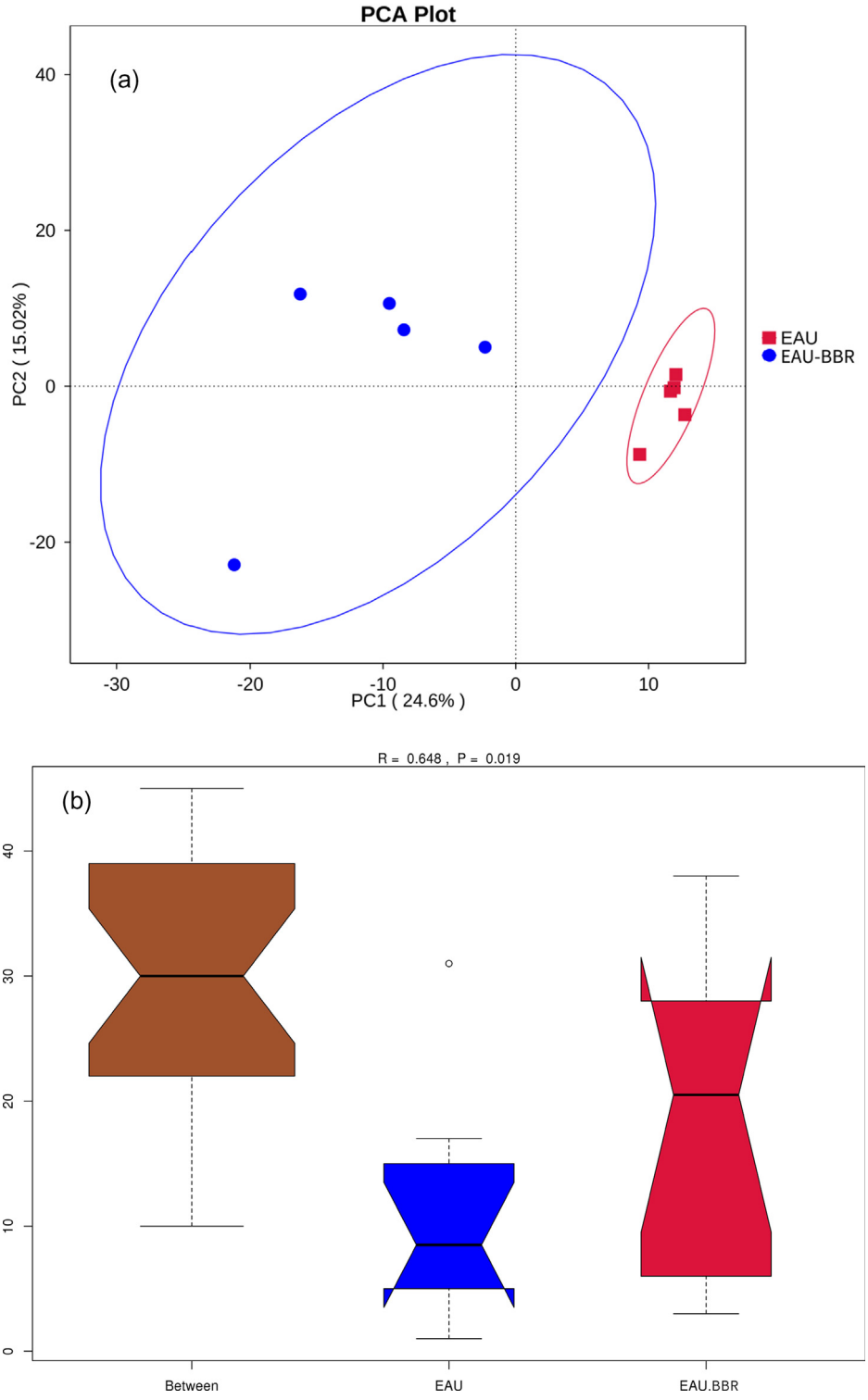

Fig. 5. Feces bacterial microbiome alterations in EAU versus EAU-BBR group. (A) Beta diversity as shown on a PCA plot. (B) The ANOSIM analysis revealed significant differences in the structure (ANOSIM, r = 0.648, P = 0.019) of gut microbiota between EAU and EAU-BBR groups. (C) LefSe analysis showing differentially abundant cecal bacterial strains in EAU mice compared to EAU-BBR mice.(D) Cladogram showing phylotype differences between EAU versus EAU-BBR mice.

we validated the mRNA expression of five genes including H2-D1, Hist1h3e, Tfrc, Zbtb16 and Ddit3 by RT-PCR. These five genes were selected from the downregulated DEGs, and they were not only enriched in the significantly down-regulated GO terms, but also in the significantly down-regulated KEGG pathways. Since few genes are significantly enriched in upregulated GO terms and KEGG pathways, all of the validated genes were selected from the downregulated DEGs. The chosen genes are shown in Table 1. RT-PCR confirmed that these genes were significantly downregulated following BBR treatment of EAU mice (Fig. 4).

3.4. BBR altered the gut microbiota composition in EAU mice.

The composition of the gut microbiota plays an important role in the

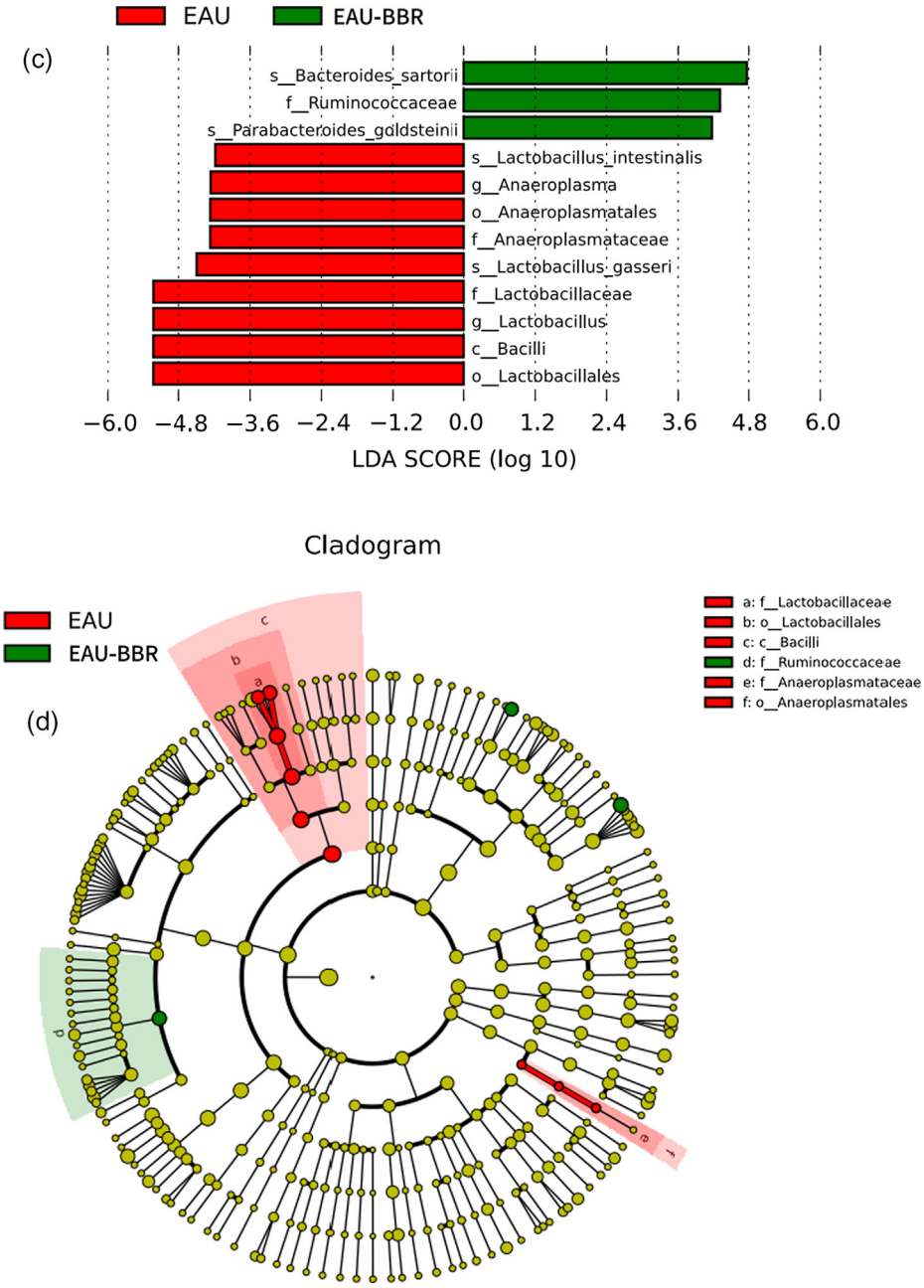

Fig. 5. (*continued*)

development of EAU [25]. To study the effect of BBR treatment on gut microbiota composition, we analyzed mouse feces 16S rRNA sequencing of mice feces, A total of 794,950 clean reads were obtained from 10 fecal samples, with a mean of 79,495 ± 1755.91 reads (range, 39,597–64,520) per subject. A total of 634 OTUs were identified. Overall, at the family taxonomic rank, *Lactobacillaceae* was the dominant microbiome in EAU group, while *Muribaculaceae* was the dominant microbiome in EAU-BBR group. At the genus level, *Lactobacillus* was the major microbiome in EAU group, while *Bacteroides* was the major microbiome in EAU-BBR group (Fig. S1). The Shannon indexes and Simpson index showed the alpha diversity had no significant difference between the EAU group and EAU-BBR group mice after 2 weeks BBR treatment (Fig. S2). To determine the similarity of microbiota communities, PCA was performed. Results showed that the gut microbiota from the EAU and EAU-BBR groups divided into two different parts that were distinct in the PCA (Fig. 5A), suggesting that intestinal microbiota were altered by BBR treatment in EAU. The ANOSIM analysis revealed significant differences in the structure (ANOSIM, $r = 0.648$, $P = 0.019$) of gut microbiota between EAU and EAU-BBR groups (Fig. 5B).

We subsequently compared the differences in taxonomic abundances between EAU and BBR-EAU groups by using LefSe and MetaStat analysis. LefSe analysis revealed that 3 bacterial taxa were enriched in EAU-BBR group and 9 bacterial taxa were enriched in the EAU group (Fig. 5B). The resulting cladogram showed that the family of *Ruminococcaceae* had a large effect size in the EAU-BBR group. The class *Bacilli*, the order *Anaeroplasmatales* and *Lactobacillales*, the family *Anaeroplasmataceae* and *Lactobacillaceae* was predominant in the EAU group (Fig. 5C). Using MetaStat analysis, we found that five genera were reduced in mice after BBR treatment including *Lactobacillus*, whereas thirteen genera were increased in the BBR-EAU group including *Akkermansia* and *Oscillibacter* (Table S2).

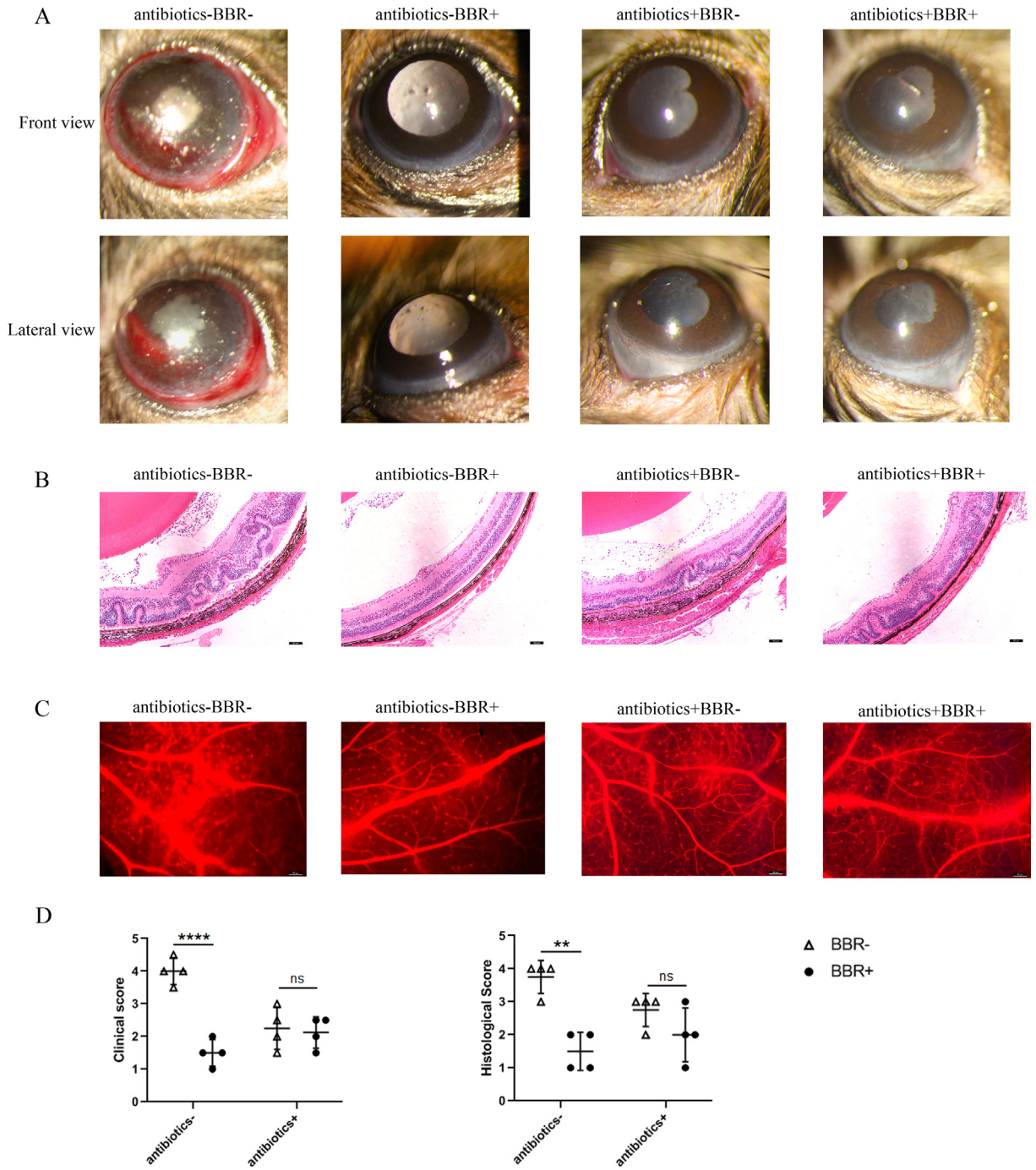

Fig. 6. Ocular evaluation of EAU mice: Depletion of gut microbiota affected the efficacy of BBR on clinical scores, histological scores and BRB breakdown in EAU. (A) Representative slit-lamp images of eye sections in antibiotics-BBR-, antibiotics-BBR+, antibiotics+BBR-, antibiotics+BBR+ groups mice. (B) Representative hematoxylin and eosin images of eye sections from antibiotics-BBR-, antibiotics-BBR+, antibiotics+BBR-, antibiotics+BBR+ groups mice. (C) Representative Evans blue images of retinas from antibiotics-BBR-, antibiotics-BBR+, antibiotics+BBR-, antibiotics+BBR+ groups mice. Scale bar, 80 μm (n = 4/group). (D) Quantification of clinical scores and histopathological scores. (n = 4/group; mean ± SD; ****p < 0.0001; **p < 0.01; Two-way ANOVA with Tukey multiple comparisons test). Representative data from 2 to 3 independent experiments. (For interpretation of the references to colour in this figure legend, the reader is referred to the web version of this article.)

3.5. Depletion of gut microbiota affected the efficacy of BBR on EAU.

To identify the role of gut microbiota following BBR treatment, mice were randomly divided into four groups: antibiotics-BBR-, antibiotics-BBR+, antibiotics+BBR-, antibiotics+BBR+. Before induction of EAU and treatment with BBR, the antibiotics+BBR- and antibiotics+BBR+ groups mice were treated with a combination of antibiotics to deplete the gut microbiota.

The results showed that following EAU induction, the antibiotics-BBR+ showed significantly decreased clinical scores, histological scores, and attenuated BRB breakdown of EAU, which is consistent with the earlier observations shown above. No significant differences between clinical scores, histological scores, and BRB breakdown in antibiotics+BBR- treated mice was observed when comparing antibiotics+BBR+ treated mice (Fig. 6A–C).

In addition, IFN-γ and IL-17 levels were decreased in retinal tissue

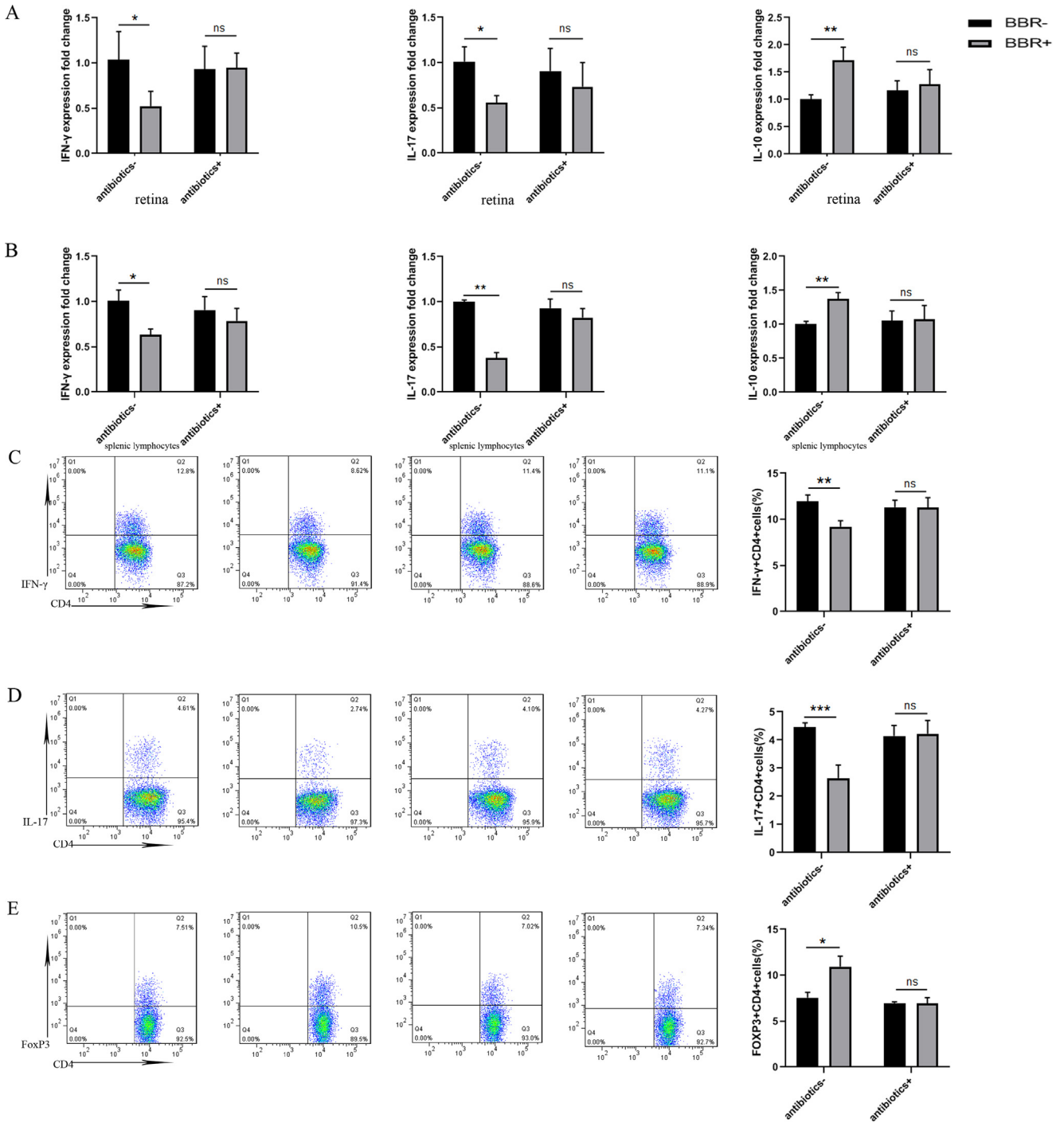

Fig. 7. BBR treatment does not influence effector and regulatory T cell balance after depletion of gut microbiota. (A) The mRNA expression of IFN-γ, IL-17, IL-10 were detected by real-time PCR in retina from antibiotics-BBR-, antibiotics-BBR+, antibiotics + BBR-, antibiotics + BBR+ groups mice. (n = 4/group; mean ± SD; ** $p < 0.01$, *$p < 0.05$; Two-way ANOVA with Tukey multiple comparisons test). (B) The mRNA expression of IFN-γ, IL-17, IL-10 were detected by real-time PCR in splenic lymphocytes from antibiotics-BBR-, antibiotics-BBR+, antibiotics + BBR-, antibiotics + BBR+ groups mice. (n = 4/group; mean ± SD; ** $p < 0.01$, *$p < 0.05$; Two-way ANOVA with Tukey multiple comparisons test). (C)(D)(E) Representative and quantification of IFN-γ + CD4+ T cells, IL-17A + CD4+ T cells and CD4 + Foxp3+ cells in the splenic lymphocytes of antibiotics-BBR-, antibiotics-BBR+, antibiotics + BBR-, antibiotics + BBR+ groups mice. (n = 4/group; mean ± SD; ***$p < 0.001$, ** $p < 0.01$; Two-way ANOVA with Tukey multiple comparisons test). Representative data from 2 to 3 independent experiments.

and splenic lymphocytes whilst IL-10 levels were increased in antibiotics-BBR+ treated mice compared with antibiotics-BBR- treated mice, whereas there were no obvious difference in retinal tissue and splenic lymphocyte expression of IFN-γ, IL-17 and IL-10 in antibiotics + BBR- treated mice compared with antibiotics + BBR+ treated mice (Fig. 7A and B). Th1 and Th17 cells in spleen lymphocytes were decreased whilst Treg cells were increased in antibiotics-BBR+ treated mice compared with antibiotics-BBR+ treated mice, whereas there were no obvious difference in the Th1, Th17 and Treg cell ratio in spleen lymphocytes in antibiotics + BBR- treated mice compared with antibiotics + BBR+ treated mice (Fig. 7C–E).

3.6. Correlation analysis of RNA-seq and gut microbiota composition

To investigate whether DEGs expression was associated with differential gut microbiota we analyzed our data using Spearman correlation analysis. *Lactobacillus* was positively correlated with Hist1h1a, Hist1h1e, Hist1h1d, Hist1h1b and Hist1h2bg ($P = 0.0027$, $r = 1$), *Akkermansia* was negatively correlated with Hist1h4h and Hist1h3e ($P = 0.0027$, $r = -1$), *Oscillibacter* was negatively correlated with Hist1h4c, Hist1h2ai ($P = 0.0167$, $r = -0.9429$) and Hist1h2af ($P = 0.0333$, $r = -0.8857$) (Supplemental Material 2).

4. Discussion

This study shows that treatment with BBR can block EAU and that this is accompanied by a reduced frequency of pathogenic splenic Th1 and Th17 cells and a small increase of regulatory T cells (Tregs). These findings are in agreement with earlier studies showing the role of these T cell populations in the pathogenesis of uveitis [26,27].

Our study confirms earlier preliminary data on the role of BBR on EAU and Experimental Autoimmune Encephalomyelitis (EAE) in rats and has expanded these findings by addressing the role of gene expression and gut microbiota associated with this specific treatment [11,28]. To thoroughly explore the systemic immunomodulatory effects of BBR, the expression of genes in the spleen, which is the largest immune organ, was measured using RNA-seq technology. To the best of our knowledge, this is the first study on gene expression profiling in EAU mice treated with BBR. The results showed that treatment with BBR was associated with marked changes in spleen gene transcription profiles. Analysis of GO functional classification, as well as KEGG pathway enrichment analysis, showed that BBR treatment greatly influences genes belonging to chromatin remodeling and immune-related pathways. This approach may help to discover novel molecular mechanisms whereby BBR treatment affects EAU. H2-D1, Hist1h3e, Zbtb16, Tfrc, Ddit3 were markedly enriched in both GO terms and KEGG pathways and their functions are briefly described in the following section. The most significant DEGs identified in the present study was a cluster of MHC genes, including H2-D1. The MHC plays an essential role in presenting antigens to T cells [29]. Tissue-invading autoreactive Th1 and Th17 cells require MHC antigens for their reactivation in the organ, and lower levels of MHC will decrease expression of proinflammatory cytokines [30]. We also observed a dramatically decreased expression of several histones, including Hist1h3e, which form the basic units of chromatin [31]. Circulating histones are the main cytotoxic components of neutrophil extracellular traps (NETs), which were recently proven to cause endothelial damage, proinflammatory cytokine release, induction and expansion of autoreactive Th cells, and were recently identified as the pivotal mediators of distant organ damage in systemic inflammatory diseases including uveitis [32–34]. Transferrin receptors (TFRs) are encoded by TfRc, which is a membrane glycoprotein, which can import iron [35]. In macrophages, inflammatory signals can activate TFR expression [36]. Additionally, TFR-mediated iron uptake is also essential for T cells development and proliferation [37,38]. ZBTB16/PLZF is a transcription factor involved in regulating various biological processes, including myeloid differentiation as well as the differentiation of naive T cells into effector T cells [39,40]. DDIT3 is an ER stress marker, which is expressed following a range of stress stimuli, including inflammation [41]. In the current study we found that the expression of the five genes mentioned above were markedly reduced in the BBR-treated mice, indicating that these genes may contribute to the treatment effect of BBR in EAU.

Several studies have demonstrated that gut microbiota imbalance may have an impact on the development of autoimmune disease including uveitis [25]. The effect of BBR on intestinal microbiota has not yet been reported earlier and although the alpha diversity of gut microbiota between the EAU and BBR-EAU group showed no significant changes, significant differences in microbiota composition were revealed following analysis of PCA plots and ANOSIM analysis. Microbiota composition and diversity were analyzed using MetaStat, LefSe. The class *Bacilli* and *Lactobacillaceae*, a family of lactic acid bacteria, were shown to cause an increased type I IFN gene expression in the spleen and to worsen autoimmune manifestations. Moreover, these bacterial strains have been shown to be involved in the pathogenesis of both EAU in mice as well as in BD patients [42–44]. In our study, two genera of the *Lactobacillaceae* family were shown to be reduced after BBR treatment. It is known that *Lachnospiraceae* and *Ruminococcaceae* are mainly butyrate producing bacteria and were shown to be able to increase the Treg/Th17 ratio [45,46]. The genera *Akkermansia* was enriched in our EAU-BBR group and other studies have shown that these bacteria can mediate negative effects of IFN-γ and protect against metabolic syndrome and are able to attenuate insulin resistance [47]. *Oscillibacter* was found to be increased after BBR treatment in the present study, and is a known producers of pentanoate and capable of enhancing the differentiation of Tregs [46,48]. Taken together these data suggest that gut microbiota can participate in the therapeutic effect of BBR, eventually leading to a beneficial regulatory T cell balance during EAU.

We also investigated whether gut microbiota play a role in the efficacy of BBR in EAU. The depletion of gut microbiota through combined antibiotics treatment is widely used to research the role of intestinal microbiota [49]. In our study. It was observed that BBR did not markedly affect EAU following depletion of gut microbiota, and BBR treatment did not influence the effector and regulatory T cell balance after depletion of gut microbiota. Taken together these findings suggest that gut microbiota composition plays an important role during EAU treatment as affects the efficacy of BBR.

It has been shown that gut microbiota composition correlates with altered gene expression in host tissues [50,51]. Our previous studies showed that transplantation of feces from patients with uveitis to mice, increased the severity of EAU and increased gene expression of IL-17 and IFN-γ in the EAU spleen [52]. In the present study, we examined whether spleen gene expression was associated with differential gut microbiota composition. As mentioned above, treatment of EAU mice with BBR, was associated with a markedly decreased expression of histone family member genes that are involved in NETs formation [53]. The level of circulating histones or NETs are increased in uveitis patients and can lead to endothelial cytotoxicity and vasculitis [34]. Moreover, recent studies have described that intestinal microbes might be able to regulate neutrophil functions, including the capacity of NETs formation [54]. This is supported by our observation that *Lactobacillus*, *Akkermansia* and *Oscillibacter* were correlated with histone gene expression. We assume that cross-talk between the gut microbiota and the host immune system may influence the efficacy of BBR in EAU.

Our study described a potential therapeutic effect of BBR for the treatment of uveitis. A limitation of our study is the fact that we only tested the efficacy of the drug at one time point (day 14: peak point of disease activity) after IRBP peptide immunization and drug treatment. It would be interesting to study the effect of BBR on a chronic recurrent uveitis model and begin treatment once EAU has developed, since this would mimic the normal situation in a clinical setting where patients are treated when they come into the hospital with clinical signs of uveitis. In a preliminary experiment we treated mice with BBR from day 11 (onset of disease) up to day 14 (peak of disease) after EAU induction. BBR did not show a therapeutic effect in this short-term treatment experiment (data not shown). Clinical uveitis is usually chronic and recurrent, whether EAU is an acute and self-limited disease model. There is currently not a good animal model of chronic recurrent uveitis. When such models become available we will further study the effects of berberine in chronic recurrent uveitis. Further longitudinal studies are also needed to examine the effects of BBR on EAU development with time in more detail. Additionally, to significantly improve bioavailability and efficacy of BBR, many kinds of new BBR deliveries including BBR nanoparticles were recently invented, and it would be interesting

to apply these innovations to uveitis treatment [55].

No toxicity studies were done and it is not sure whether the dose of BBR used in our study in mice is effective to control inflammation in humans without the occurrence of side effects. Earlier in vitro studies from our laboratory using BBR showed that it blocked the expression of inflammatory cytokines by a cell line of human retinal pigment epithelial cells and that it could suppress the Th17 response in Vogt Koyanagi Harada uveitis patients. At the time of writing 62 clinical trials with BBR were listed on the clinical trials registry (https://clinicaltrials.gov/; October 12, 2019), although none addressed the treatment of eye disease.

In summary, we showed that BBR treatment can block ocular manifestations of EAU by altering the balance between effector and regulatory T cells, which was associated with a significant change in the spleen transcriptome and intestinal microbial composition. We also found that gut microbiota play an important role during EAU treatment as it affects the efficacy of BBR. Taken together, these findings suggest that BBR may be a potential therapeutic drug for the treatment of uveitis.

CRediT authorship contribution statement

Ziyu Du: Conceptualization, Methodology, Writing - original draft, Investigation, Formal analysis, Validation, Project administration. **Qingfeng Wang:** Validation, Formal analysis, Investigation. **Xinyue Huang:** Validation, Formal analysis. **Shenglan Yi:** Validation, Formal analysis. **Suyin Mei:** Formal analysis, Investigation. **Gangxiang Yuan:** Investigation. **Guannan Su:** Project administration. **Qingfeng Cao:** Data curation. **Chunjiang Zhou:** Resources, Visualization. **Yao Wang:** Resources. **Aize Kijlstra:** Writing - review & editing. **Peizeng Yang:** Conceptualization, Writing - review & editing, Supervision, Funding acquisition.

Acknowledgement

This study was supported by Research fund for Traditional Chinese Medicine of Chongqing Health and Family Planning Commission (ZY20141013), Natural Science Foundation Major International (Regional) Joint Research Project (81720108009), Chongqing Key Laboratory of Ophthalmology (CSTC, 2008CA5003), Chongqing Science & Technology Platform and Base Construction Program (cstc2014pt-sy10002), the Natural Science Foundation Project of Chongqing (cstc2017shmsA130073) and National Natural Science Foundation Key Program (81930023).

Appendix A. Supplementary material

Supplementary data to this article can be found online at https://doi.org/10.1016/j.intimp.2020.106270.

References

[1] A. Rothova, H.J. Buitenhuis, C. Meenken, et al., Uveitis and systemic disease, British J. Ophthalmol. 76 (1992) 137–141, https://doi.org/10.1136/bjo.76.3.137.
[2] J.J. Servat, K.A. Mears, E.H. Black, J.J. Huang, Biological agents for the treatment of uveitis, Expert Opin. Biol. Ther. 12 (2012) 311–328.
[3] M. Gomes Bittencourt, Y.J. Sepah, D.V. Do, et al., New treatment options for non-infectious uveitis, Dev. Ophthalmol. 51 (2012) 134–161.
[4] R.R. Caspi, F.G. Roberge, C.C. Chan, et al., A new model of autoimmune disease. Experimental autoimmune uveoretinitis induced in mice with two different retinal antigens, J. Immunol. (Baltimore, Md.: 1950) 140 (1988) 1490–1495.
[5] H.R. Jiang, L. Lumsden, J.V. Forrester, Macrophages and dendritic cells in IRBP-induced experimental autoimmune uveoretinitis in B10RIII mice, Invest. Ophthalmol. Vis. Sci. 40 (1999) 3177–3185.
[6] R.R. Caspi, A look at autoimmunity and inflammation in the eye, J. Clin. Investig. 120 (2010) 3073–3083.
[7] R. Horai, R.R. Caspi, Cytokines in autoimmune uveitis, J. Interferon Cytokine Res.: Off. J. Int. Soc. Interferon Cytokine Res. 31 (2011) 733–744.
[8] W. Kong, J. Wei, P. Abidi, et al., Berberine is a novel cholesterol-lowering drug working through a unique mechanism distinct from statins, Nat. Med. 10 (2004) 1344–1351, https://doi.org/10.1038/nm1135.
[9] H. Li, X.L. Li, M. Zhang, et al., Berberine ameliorates experimental autoimmune neuritis by suppressing both cellular and humoral immunity, Scand. J. Immunol. 79 (2014) 12–19.
[10] H. Cui, Y. Cai, L. Wang, et al., Berberine regulates treg/Th17 balance to treat ulcerative colitis through modulating the gut microbiota in the colon, Front. Pharmacol. 9 (2018) 571.
[11] X. Qin, B.T. Guo, B. Wan, et al., Regulation of Th1 and Th17 cell differentiation and amelioration of experimental autoimmune encephalomyelitis by natural product compound berberine, J. Immunol. (Baltimore, Md.: 1950) 185 (2010) 1855–1863.
[12] Y. Yang, Q. Wang, M. Xie, et al., Berberine exerts an anti-inflammatory role in ocular Behcet's disease, Mol. Med. Rep. 15 (2017) 97–102.
[13] Y. Yang, J. Qi, Q. Wang, et al., Berberine suppresses Th17 and dendritic cell responses, Invest. Ophthalmol. Vis. Sci. 54 (2013) 2516–2522.
[14] L. Tian, P. Yang, B. Lei, et al., AAV2-mediated subretinal gene transfer of hIFN-α attenuates experimental autoimmune uveoretinitis in mice, PloS one 6 (2011) e19542.
[15] R.R. Caspi, Experimental autoimmune uveoretinitis in the rat and mouse, Curr. Protoc. Immunol. Unit 15 (16) (2003).
[16] D.A. Copland, J. Liu, L.P. Schewitz-Bowers, et al., Therapeutic dosing of fingolimod (FTY720) prevents cell infiltration, rapidly suppresses ocular inflammation, and maintains the blood-ocular barrier, Am. J. Pathol. 180 (2012) 672–681.
[17] Lydia Tesfa, Franz-Wilhelm Koch, Wulf Pankow, Hans-Dieter Volk, Florian Kern, Confirmation ofMycobacterium tuberculosis infection by flow cytometry after ex vivo incubation of peripheral blood T cells with an ESAT-6-derived peptide pool, Cytometry 60B (1) (2004) 47–53, https://doi.org/10.1002/(ISSN)1097-032010.1002/cyto.b.v60b:110.1002/cyto.b.20007.
[18] M.K. Maropola, J.B. Ramond, M. Trindade, Impact of metagenomic DNA extraction procedures on the identifiable endophytic bacterial diversity in Sorghum bicolor (L. Moench), J. Microbiol. Methods 112 (2015) 104–117.
[19] P.F. Kemp, J.Y. Aller, Bacterial diversity in aquatic and other environments: what 16S rDNA libraries can tell us, FEMS Microbiol. Ecol. 47 (2004) 161–177.
[20] R.C. Edgar, B.J. Haas, J.C. Clemente, C. Quince, R. Knight, UCHIME improves sensitivity and speed of chimera detection, Bioinform. (Oxford, England) 27 (2011) 2194–2200.
[21] R.C. Edgar, UPARSE: highly accurate OTU sequences from microbial amplicon reads, Nat. Methods 10 (2013) 996–998.
[22] C. Quast, E. Pruesse, P. Yilmaz, et al., The SILVA ribosomal RNA gene database project: improved data processing and web-based tools, Nucleic Acids Res. 41 (2013) D590–D596.
[23] N. Segata, J. Izard, L. Waldron, et al., Metagenomic biomarker discovery and explanation, Genome Biol. 12 (2011) R60.
[24] J.R. White, N. Nagarajan, M. Pop, Statistical methods for detecting differentially abundant features in clinical metagenomic samples, PLoS computational biology 5 (2009) e1000352.
[25] R. Horai, C.R. Zárate-Bladés, P. Dillenburg-Pilla, et al., Microbiota-dependent activation of an autoreactive T cell receptor provokes autoimmunity in an immunologically privileged site, Immunity 43 (2015) 343–353.
[26] D. Luger, P.B. Silver, J. Tang, et al., Either a Th17 or a Th1 effector response can drive autoimmunity: conditions of disease induction affect dominant effector category, J. Exp. Med. 205 (2008) 799–810.
[27] R. Caspi, Autoimmunity in the immune privileged eye: pathogenic and regulatory T cells, Immunol. Res. 42 (2008) 41–50.
[28] M. Li, X. Chen, J. Liu, et al., Treatment of experimental autoimmune uveoretinitis with different natural compounds, Mol. Med. Rep. 13 (2016) 4654–4658.
[29] W.K. Potts, P.R. Slev, Pathogen-based models favoring MHC genetic diversity, Immunol. Rev. 143 (1995) 181–197, https://doi.org/10.1111/j.1600-065x.1995.tb00675.x.
[30] D. Hertzenberg, K. Lehmann-Horn, S. Kinzel, et al., Developmental maturation of innate immune cell function correlates with susceptibility to central nervous system autoimmunity, Eur. J. Immunol. 43 (2013) 2078–2088, https://doi.org/10.1002/eji.201343338.
[31] N. Happel, D. Doenecke, Histone H1 and its isoforms: contribution to chromatin structure and function, Gene 431 (2009) 1–12.
[32] Z. Wen, Z. Lei, L. Yao, et al., Circulating histones are major mediators of systemic inflammation and cellular injury in patients with acute liver failure, Cell Death Dis. 7 (2016) e2391, https://doi.org/10.1038/cddis.2016.303.
[33] G. Papadaki, K. Kambas, C. Choulaki, et al., Neutrophil extracellular traps exacerbate Th1-mediated autoimmune responses in rheumatoid arthritis by promoting DC maturation, Eur. J. Immunol. 46 (2016) 2542–2554, https://doi.org/10.1002/eji.201646542.
[34] R. Safi, R. Kallas, T. Bardawil, et al., Neutrophils contribute to vasculitis by increased release of neutrophil extracellular traps in Behçet's disease, J. Dermatol. Sci. 92 (2018) 143–150, https://doi.org/10.1016/j.jdermsci.2018.08.010.
[35] A. Lopez, P. Cacoub, I.C. Macdougall, L. Peyrin-Biroulet, Iron deficiency anaemia, Lancet (London, England) 387 (2016) 907–916.
[36] S.Q. Jing, T. Spencer, K. Miller, C. Hopkins, I.S. Trowbridge, Role of the human transferrin receptor cytoplasmic domain in endocytosis: localization of a specific signal sequence for internalization, J. Cell Biol. 110 (1990) 283–294.
[37] L.M. Neckers, J. Cossman, Transferrin receptor induction in mitogen-stimulated human T lymphocytes is required for DNA synthesis and cell division and is regulated by interleukin 2, Proc. Natl. Acad. of Sci. U.S.A. 80 (1983), https://doi.org/10.1073/pnas.80.11.3494.
[38] R.M. Ned, W. Swat, N.C. Andrews, Transferrin receptor 1 is differentially required in lymphocyte development, Blood 102 (2003) 3711–3718, https://doi.org/10.1182/blood-2003-04-1086.

[39] T.M. Liu, E.H. Lee, B. Lim, N. Shyh-Chang, Concise review: balancing stem cell self-renewal and differentiation with PLZF, Stem Cells (Dayton, Ohio) 34 (2016) 277–287.
[40] E.S. Alonzo, D.B. Sant'Angelo, Development of PLZF-expressing innate T cells, Curr. Opin. Immunol. 23 (2011) 220–227.
[41] A. Coope, L.B. Pascoal, J.D. Botezelli, et al., ER stress activation in the intestinal mucosa but not in mesenteric adipose tissue is associated with inflammation in Crohn's disease patients, PloS One 14 (2019) e0223105.
[42] J. Shimizu, T. Kubota, E. Takada, et al., Bifidobacteria abundance-featured gut microbiota compositional change in patients with Behcet's disease, PloS One 11 (2016) e0153746.
[43] C. Janowitz, Y.K. Nakamura, C. Metea, et al., Disruption of intestinal homeostasis and intestinal microbiota during experimental autoimmune uveitis, Invest. Ophthalmol. Vis. Sci. 60 (2019) 420–429.
[44] D.F. Zegarra-Ruiz, A. El Beidaq, A.J. Iñiguez, et al., A diet-sensitive commensal lactobacillus strain mediates TLR7-dependent systemic autoimmunity, Cell Host Microbe 25 (2019), https://doi.org/10.1016/j.chom.2018.11.009 113-127.e116.
[45] M. Vital, A. Karch, D.H. Pieper, Colonic butyrate-producing communities in humans: an overview using omics data, mSystems 2 (2017), https://doi.org/10.1128/mSystems.00130-17.
[46] N. Arpaia, C. Campbell, X. Fan, et al., Metabolites produced by commensal bacteria promote peripheral regulatory T-cell generation, Nature 504 (2013) 451–455, https://doi.org/10.1038/nature12726.
[47] R.L. Greer, X. Dong, A.C. Moraes, et al., Akkermansia muciniphila mediates negative effects of IFNγ on glucose metabolism, Nat. Commun. 7 (2016) 13329, https://doi.org/10.1038/ncomms13329.
[48] J. Li, C.Y. Sung, N. Lee, et al., Probiotics modulated gut microbiota suppresses hepatocellular carcinoma growth in mice, Proc. Natl. Acad. Sci. U.S.A. 113 (2016) E1306–E1315.
[49] E. Elinav, T. Strowig, A.L. Kau, et al., NLRP6 inflammasome regulates colonic microbial ecology and risk for colitis, Cell 145 (2011) 745–757, https://doi.org/10.1016/j.cell.2011.04.022.
[50] J.O. Alemán, N.A. Bokulich, J.R. Swann, et al., Fecal microbiota and bile acid interactions with systemic and adipose tissue metabolism in diet-induced weight loss of obese postmenopausal women, J. Trans. Med. 16 (2018) 244, https://doi.org/10.1186/s12967-018-1619-z.
[51] S. Pellegrini, V. Sordi, A.M. Bolla, et al., Duodenal mucosa of patients with type 1 diabetes shows distinctive inflammatory profile and microbiota, J. Clin. Endocrinol. Metab. 102 (2017) 1468–1477, https://doi.org/10.1210/jc.2016-3222.
[52] Z. Ye, N. Zhang, C. Wu, et al., A metagenomic study of the gut microbiome in Behcet's disease, Microbiome 6 (2018) 135, https://doi.org/10.1186/s40168-018-0520-6.
[53] S.T. Abrams, N. Zhang, J. Manson, et al., Circulating histones are mediators of trauma-associated lung injury, Am. J. Respir. Crit. Care Med. 187 (2013) 160–169, https://doi.org/10.1164/rccm.201206-1037OC.
[54] L. Vong, C.W. Yeung, L.J. Pinnell, P.M. Sherman, Adherent-invasive escherichia coli exacerbates antibiotic-associated intestinal dysbiosis and neutrophil extracellular trap activation, Inflamm. Bowel Dis. 22 (2016) 42–54, https://doi.org/10.1097/mib.0000000000000591.
[55] H.H. Guo, C.L. Feng, W.X. Zhang, et al., Liver-target nanotechnology facilitates berberine to ameliorate cardio-metabolic diseases, Nat. Commun. 10 (2019) 1981, https://doi.org/10.1038/s41467-019-09852-0.